Fluid and gyrokinetic simulations of plasmoid formation in collisionless plasmas

C. Granier[1,2], D. Borgogno[2], L. Comisso[3], D. Grasso[2], R. Numata[4], E. Tassi[1]

[1] *Université Côte d'Azur, CNRS, Observatoire de la Côte d'Azur, Laboratoire J. L. Lagrange, Boulevard de l'Observatoire, CS 34229, 06304 Nice Cedex 4, France*

[2] *Istituto dei Sistemi Complessi - CNR and Dipartimento di Energia, Politecnico di Torino, Torino 10129, Italy*

[3] *Department of Astronomy and Columbia Astrophysics Laboratory, Columbia University, New York, New York 10027, USA*

[4] *Graduate School of Simulation Studies, University of Hyogo, Kobe 650-0047, Japan*

Introduction

The instabilities of thin current sheets that lead to the formation of plasmoids have been greatly studied (see, e.g. Refs. [1, 2]) and were shown to play an important role for achieving large reconnection rates.

In this proceeding paper, we investigate the plasmoid formation employing both fluid and gyrokinetic simulations, assuming a plasma with cold ions that is immersed in a strong guide field, resulting in low plasma β_e. We present simulations of a marginally stable collisionless current sheet, formed after the tearing instability. We focus on two different regimes, $\rho_s \ll d_e$ and $\rho_s \gg d_e$, where $\rho_s = \frac{1}{L}\sqrt{\frac{T_{0e}}{m_i}}\frac{m_i c}{eB_0}$ and $d_e = \frac{1}{L}c\sqrt{\frac{m_e}{4\pi e^2 n_0}}$, correspond to the normalized sonic Larmor radius and electron skin depth, respectively, and L is the characteristic equilibrium scale length.

Set up

The fluid model is the cold ion Larmor radius limit of the model derived in [3], and retains electron inertia. Specifically, the equations governing the plasma dynamics are

$$\frac{\partial n_e}{\partial t} + [\phi, n_e] = [A_\parallel, u_e]\,, \tag{1}$$

$$\frac{\partial}{\partial t}\left(A_\parallel - d_e^2 u_e\right) + \left[\phi, A_\parallel - d_e^2 u_e\right] = \rho_s^2 [n_e, A_\parallel]\,, \tag{2}$$

where $A_\parallel$ and ϕ are the magnetic and electrostatic potential, normalized as $A_\parallel = \hat{A}_\parallel/(LB_0)$ and $\phi = c\hat{\phi}/(v_A L B_0)$, where $n_e = \nabla_\perp^2 \phi$ is the electron density perturbation, and $u_e = \nabla_\perp^2 A_\parallel$ is the parallel electron velocity, also proportional to the current density. The time and spatial variables are normalized as $t = v_A \hat{t}/L$ and $x = \hat{x}/L$, where v_A is the Alfvén velocity. We consider a slab

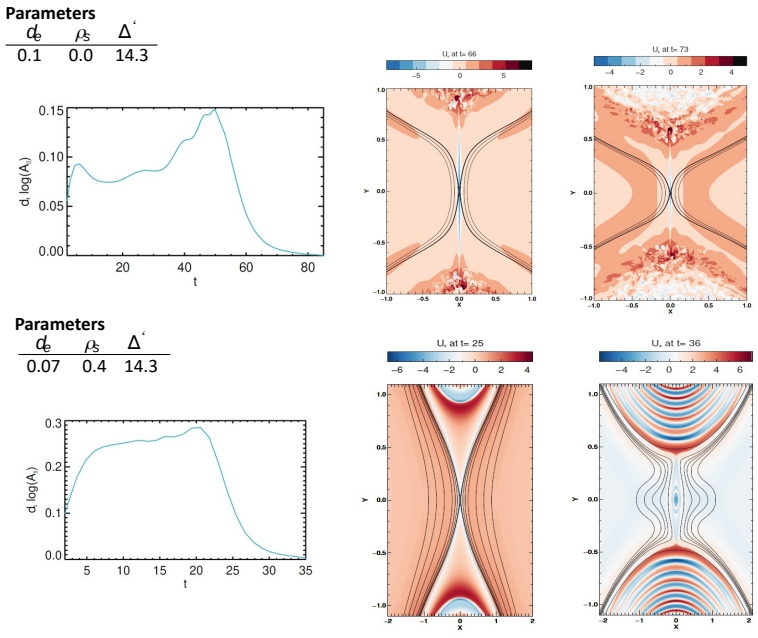

Figure 1: Growth rate evolution and contour plot of the parallel current density with iso-potential lines for, $d_e = 0.1$ and $\rho_s = 0.0$ (top) and $d_e = 0.07$ and $\rho_s = 0.4$ (bottom). The number of grid points is 1728×1728.

geometry in which the magnetic field is given by $\mathbf{B} \approx \hat{z} + \nabla A_{\parallel} \times \hat{z}$. The perpendicular flow velocity is given by $\mathbf{u}_{\perp} = \hat{z} \times \nabla \phi$. In Eqs. (1) and (2), $[f,g] = \partial_x f \partial_y g - \partial_y f \partial_x g$.

We performed 2D simulations in a slab geometry. We assume a tearing equilibrium given by $\phi^{(0)}(x) = 0$, $A_{\parallel}^{(0)}(x) = A_0/\cosh^2(x)$. The tearing parameter for this equilibrium is $\Delta'_{box} = 2\left(5 - k_y^2\right)\left(k_y^2 + 3\right)/(k_y^2(k_y^2+4)^{1/2})$.

The fluid model (1) and (2) allowed to determine a plasmoid regime [4] (preprint available at `https://arxiv.org/abs/2206.06412`). Figure 1 shows two simulations for which the current sheet is at a state of marginal stability and confirms the results obtained in the preprint [4] i.e, that the regime $\rho_s \gg d_e$ promotes the onset of plasmoids. On Fig. 1 we can see that, if electron inertia dominates, an elongated current sheet develops from the ideal fluid motion. On the other hand, when the ion-sound Larmor radius is significantly large compared to the electron skin depth, the shape of the current layer is notably affected and follows the separatrices. As will be shown, taking into account the ion-sound Larmor radius effects (which corresponds to including a parallel compressibility of the electrons) can promote the onset of plasmoids.

In the next section we focus on a comparison of fluid and gyrokinetic simulations of a marginally stable current sheet.

Comparisons for a marginally stable case

The gyrokinetic model, adopted for the comparison, is a δf model, from which the fluid model can be derived with appropriate approximations and closure hypotheses [5]. The gyroki-

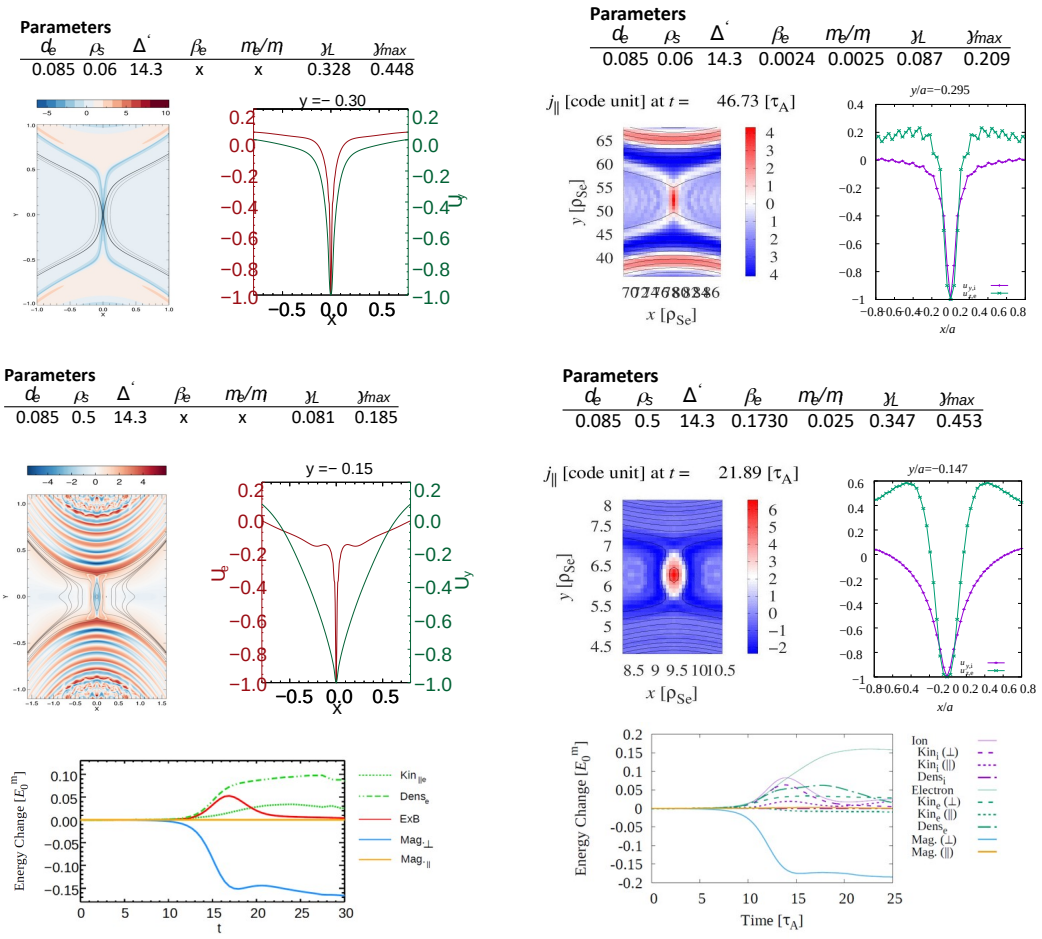

Figure 2: Left panels: fluid simulations. Right panels: gyrokinetic simulations with the same d_e and ρ_s. For the fluid case, we show the contour of the parallel electron velocity. For the gyrokinetic case, we show the contour of the current density. For each simulation we show an overplot of the profile of the parallel electron velocity u_e at $y = 0$ and of the y component of the perpendicular flow (outflow coming out of the current sheet). The outflow profile position is indicated on top of the figures and corresponds to $y \sim L_{cs}/2$. For the simulation $d_e = 0.085$ and $\rho_s = 0.5$ we also show the time evolution of the energy variations.

netic equations are solved by means of the Astro GK code, presented and used in [6, 7]. In the fluid case, the Eqs. (1) and (2) assume $\beta_e \sim m_e/m_i \sim 0$. The gyrokinetic simulations were therefore carried out with $m_e/m_i = 0.0025$ and the corresponding value of β_e is reported in the table. The temperature ratio was set to $\tau = T_{0i}/T_{0e} = 10^{-3}$, implying a ion Larmor radius of $\rho_i = \sqrt{2.10^{-3}}\rho_s$.

We compare the simulations presented in Fig. 2. This comparison makes it possible to confirm that, by simply adding bi-fluid effects resulting from a large ion-sound Larmor radius, one can switch from a marginally stable case to a marginally unstable case, even when it implies that the plasma β_e increases as well. Indeed, the idea was to check if the instability threshold would change significantly when also including kinetic effects, assuming a small β_e and the small parallel ion dynamic that it brings, and which is neglected in the fluid model.

For the plasmoid unstable case, $\rho_s > d_e$, two-fluid effects lead to a decoupling of the plasma flow channel from the electric current density, and in this case we find a reconnection rate $R_{\rm rec} \sim (\delta_{\rm outf}/L_{\rm outf})^{(2)}_{\star} v_A B_{\rm up} \sim 0.1 v_A B_{\rm up}$, where $\delta_{\rm outf}$ and $L_{\rm outf}$ are the outflow velocity channel coming out from the end of the current sheet, and $B_{\rm up}$ is the reconnecting magnetic field. Figure 2 also shows the variation of the energy components of the simulation $d_e = 0.085$ and $\rho_s = 0.5$. It is possible to observe that, in the fluid and gyrokinetic cases, the decrease in time of magnetic energy is similar. The gyrokinetic perpendicular ion velocity is well represented by the fluid $\mathbf{E} \times \mathbf{B}$ velocity. On the other hand, gyrokinetic simulations show a large fraction of magnetic energy transferred to fluctuations of higher order moments.

These results contribute to shed light on collisionless reconnection mediated by the plasmoid instability, and in particular on the role of the sonic Larmor radius.

References

[1] W. Daughton, V. Roytershteyn, B. J. Albright, H. Karimabadi, L. Yin, and K. J. Bowers, Phys. Rev. Lett. 103, 065004 (2009).

[2] A. Bhattacharjee, Y.-M. Huang, H. Yang, and B. Rogers, Physics of Plasmas 16, 112102 (2009).

[3] T. J. Schep, F. Pegoraro, and B. N. Kuvshinov. Phys. Plasmas, 1:2843–2851, (1994).

[4] C. Granier, D. Borgogno, L. Comisso, D. Grasso, E, Tassi, R. Numata, submitted, preprint available at `https://arxiv.org/abs/2206.06412` (2022).

[5] C. Granier, D. Borgogno, D. Grasso, E, Tassi. Journal of Plasma Physics, 88(1), 905880111 (2022).

[6] Ryusuke Numata, Gregory G Howes, Tomoya Tatsuno, Michael Barnes, and William Dorland. 229(24):9347 – 9372, (2010).

[7] Ryusuke Numata and N. F. Loureiro. Journal of Plasma Physics, 81(2):305810201, (2015).